ϵ-EXPANSION OF THE ANISOTROPIC CRYSTAL LANDAU-GINZBURG MODEL

Samuel B. Johnson, *(MIT, Center for Theoretical Physics)*[1]
(Dated: 18 May, 2012)

The ϵ-expansion of the anisotropic crystal model is carried out to first order, involving the calculation of both first and second-order corrections in the original parameters. Careful track must be kept of which terms in the Hamiltonian corrections modify, as we immediately introduce a new parameter in the step of second-order RG. We investigate the resulting RG flows, as well as identify the critical exponents α and ν at the stable fixed point. An interesting result is that we can guess the higher order behavior of critical exponent that vanishes to first-order in ϵ.

1. Introduction

Here we deal with the renormalization of the anisotropic crystal model. This model is designed to roughly simulate the behavior of a classical magnetic field within a crystalline lattice such that magetization is either promoted or discouraged along a specific direction. This is an interesting model as it includes as special cases other commonly cited models [4] and also makes possible critical exponents that vary continuously with the angle from the special direction $\hat{e}_1$. We will first discuss the preliminary zeroth-order result from minimizing the Landau-Ginzburg free energy, as the complex nature of the phases obtained by this method warrants discussion. Our mean-field Hamiltonian is a variant of the standard n-component Landau-Ginzburg model:

$$\beta H = \int d^d x (\frac{t}{2}\vec{m}^2 + \frac{r}{2}m_1^2 + K(\nabla\vec{m})^2 + u(\vec{m}^2)^2 + vm_1^2\vec{m}^2) \tag{1}$$

This Hamiltonian has a basic Gaussian form, upon which the additions u and v can be considered perturbations; for stability purposes, u is assumed positive. The parameters r and v introduce an anisotropy along the direction of the first field component. The phase diagram obtained from minimizing this quantity is rather complicated; if we consider the case of $u = v = 0$, then there is a $t > 0$ disordered phase as well as two phases for $t < 0$: a phase with $r > 0$ ($O(n-1)$ order, in which the magnetic field ground state points in any direction in the $(n-1)-$plane orthogonal to $\hat{e}_1$), and a phase with $r < 0$ of Ising order, in which the magnetic field ground state aligns in the $\hat{e}_1$ direction. In the $r = 0$, $u, v \neq 0$ case, we have similarly ordered phases for $t < 0$, $v > 0$ or $v < 0$. In this case, we must also ensure $v \geq -u$ to avoid a ground state of infinite negative energy; in reality, higher order terms would prevent this, but it is nevertheless undesirable from the point of view of deriving phase diagrams. A more complete discussion is carried out in [1].

2. RG Treatment

We wish to understand how these results change when the scale at which we probe this system is modified. Conceptually this is necessary in order to ensure that our coarse-graining approximation is even valid in the first place. In practice, however, this is an efficient way of obtaining ν and α, via the eigenvalues of the matrix relating variations of the parameters around a fixed point to their infinitesimal changes under rescaling. We perform the first-order calculation of the correction to the critical temperature t_c, the temperature at which the susceptibility vanishes, in the appendix, where we also fix notation regarding our RG procedure. The result is

$$\begin{cases} (t+r)_c &= -\int đk \left\{ \dfrac{(4u+2v)(n-1)}{Kk^2+t+r} + \dfrac{8u+6v}{Kk^2+t} \right\} \\ t_c &= -2\int đk \left\{ \dfrac{(4u+v)(n-1)}{Kk^2+t} + \dfrac{2u+v}{Kk^2+t+r} \right\} \end{cases} \tag{2}$$

We will later interpret these as the first step towards recursion relations for the temperatures. Before proceeding to second order calculations for RG corrections to u and v, we note that the above calculations can be succinctly summarized by introducing the following notation. A fundamental vertex is denoted four solid lines joined by a dotted line, as in [1]. Its value is assigned to be $(2\pi)^d\delta(q_1+q_2+q_3+q_4)(u+\delta_{1i}v)$. When we represent the integrated-out modes σ by dashed (as opposed to dotted) lines, we can represent

[1] samj@mit.edu

the two fundamental contributions to the t, r renormalization by the second and third figures. The second

FIGURE 1. The fundamental vertex at left; to right, the two "tadpole" and "self-energy" diagrams contributing to RG flow of t and r.

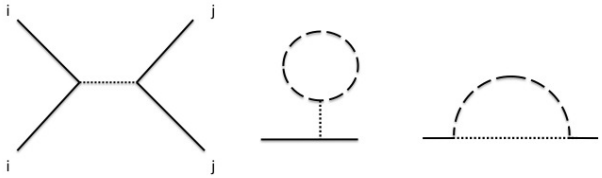

order expansion involves in principle many terms; the diagrammatic expansion provides an easy way to determine which terms are properly factors that renormalize the u or the v anisotropy parameters. Two possibilities for the box diagrams (c) are omitted from the table: they give zero contribution, showing that these interactions are not sufficient to couple different components of the fields at this order.

FIGURE 2. The three one-loop diagrams, respectively (a) - (c) from left to right, that contribute to the RG flows of u and v at second order in u and v.

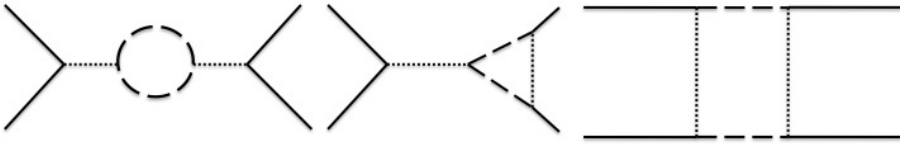

TABLE 1. Contributions from diagrams of type (a), (b), and (c), as defined in the figure. Listed as (1) - (4) are the four possibilities of left m_1, right m_1; left m_1, right other; left other, right m_1; and left and right other than m_1.

(a);1	$\frac{1}{2}\times 2\times 2\times 2\left((u+v+z)(u+v)\Delta_1^2+(u+v)u(n-1)\Delta_2^2\right)\delta l$
(a);2	$\frac{1}{2}\times 2\times 2\left((u+v+z)^2\Delta_1^2+(u+v)^2(n-1)\Delta_2^2\right)\delta l$
(a);3	$\frac{1}{2}\times 2\times 2\left((u+v+z)^2\Delta_1^2+(u+v)^2(n-1)\Delta_2^2\right)\delta l$
(a);4	$\frac{1}{2}\times 2\times 2\times 2\left((u+v)^2\Delta_1^2+u^2(n-1)\Delta_2^2\right)\delta l$
(b);1	$\frac{1}{2}\times 4\times 2\times 2(u+v+z)^2\Delta_1^2\delta l$
(b);2	$\frac{1}{2}\times 4\times 2(u+v)u\Delta_2^2\delta l$
(b);3	$\frac{1}{2}\times 4\times 2(u+v+z)(u+v)\Delta_1^2\delta l$
(b);4	$\frac{1}{2}\times 4\times 2\times 2u^2\Delta_2^2\delta l$
(c);1	$\frac{1}{2}\times 4\times 4\times 2(u+v+z)^2\Delta_1^2\delta l$
(c);4	$\frac{1}{2}\times 4\times 4\times 2(u+v+z)^2\Delta_1^2\delta l$

We have defined $\Delta_1^2 := \frac{K_d\Lambda^d}{(K\Lambda^2+t+r)^2}$ and $\Delta_2^2 := \frac{K_d\Lambda^d}{(K\Lambda^2+t)^2}$ for convenience. We have included a new parameter z, which in the Hamiltonian would appear modifying $(u+v)m_1^4 \to (u+v+z)m_1^4$. We see that although $z=0$ initially, it may becomes nonzero under renormalization because the case (1) diagrams differ from the the sum of the case (2) and (3) diagrams. For our interests, we can read off the modifications to $u+v$ from the sum of the (2) and (3) terms and u from the (4) case. Subtracting, we find $\tilde{u} = \left(20(u+v)^2\Delta_1^2 + 4u^2(n+1)\Delta_2^2\right)$ and $\tilde{v} = \left(((n-1)(2uv+v^2)+4(v-u))\Delta_2^2 - 12(u+v)^2\Delta_1^2\right)$.

Renormalization proceeds by rescaling: letting q' represents the old momentum, we introduce $qb^{-1}=q'$ so that the magnitudes of dynamical momenta lie once again between 0 and the original cutoff Λ. We also introduce z (not to be confused with the above dynamical parameter) by $m_i'(q)z = \tilde{m}_i(q')$. Substituting this into the Hamiltonian, we obtain

$$\begin{cases} t' &= b^{-d}z^2\tilde{t} \\ r' &= b^{-d}z^2\tilde{r} \\ K' &= b^{-d-2}z^2\tilde{K} \\ u' &= b^{-3d}z^4\tilde{u} \\ v' &= b^{-3d}z^4\tilde{v} \end{cases} \tag{3}$$

By demanding that short-distance behavior at the Gaussian fixed point remain unchanged, it is seen that the RG for K must be defined to be zero, hence $z = b^{d/2+1}$ and therefore at the infinitesimal level (setting $b = e^{\delta l} \approx 1 + \delta l$), we have the key expressions for u' and v' (where $\epsilon := 4 - d$):

$$\begin{cases} du/dl &= \epsilon u - \left(20(u+v)^2\Delta_1^2 + 4u^2(n+1)\Delta_2^2\right) \\ dv/dl &= \epsilon v - \left(((n-1)(2uv+v^2) + 4(v-u))\Delta_2^2 - 12(u+v)^2\Delta_1^2\right) \end{cases} \tag{4}$$

3. Results: Fixed Points and Critical Exponents

Given this work, we now have in hand the ability to calculate the relevant recursion relations. First we identify the fixed points. As expected from two (coupled) quadratic equations, there are four fixed points. Although these results are conceptually cleanest, it is greatly preferable in carrying out the solution to work with the variable $w := u + v$. (The other version, while exact, generates formulas of many pages in length.) The w equation is given by

$$\frac{dw}{dl} = \epsilon w - 4\left(7\Delta_1^2 w^2 + (n-1)\Delta_2^2 wu\right) \tag{5}$$

which immediately gives either $w = 0$ or the following relation upon u:

$$w = \frac{\epsilon/4 - u(n-1)\Delta_2^2}{7\Delta_1^2} \tag{6}$$

Substituting these into the equation for u yields the following locations for fixed points. At each location (u_*, w_*), we may define the quantities $\delta u := u - u_*$, $\delta w := w - w_*$, and linearize the matrix L relating the vector $\delta\vec{x}^T := (\delta u, \delta w)$ to its derivative under rescaling by $\frac{d}{dl}\vec{x} = L \cdot \vec{x}$; the eigenvalues of this matrix represent the critical exponents at each fixed point.

(1) *Gaussian* ($w = v = 0$) Note first that this trivially equivalent to $u = v = 0$–so this really does represent the familiar Gaussian fixed point. In this regime, all contributions to the recursion relations other than the leading terms multiplying ϵ vanish upon linearization; they all contain one of either $u_* = 0$ or $v_* = 0$. Hence the eigenvalues are determined by the dimensionality; $y_u = y_v = \epsilon$; this is unacceptable if $\epsilon > 0$, i.e. $d < 4$, for in this case we have multiple relevant directions, as opposed to only one–the "physical temperature" parameter-direction.

(2) ($w = 0; u = \frac{\epsilon}{4(n+1)\Delta_2^2}$). This point lies upon the line along which $v = -u$. We might have expected such a fixed point from the zeroth-order phase diagram considerations; this point separates physical from unphysical configurations, those that are not bounded below energetically. This fixed point turns out to be the most subtle; at this order in ϵ, $y_v = \epsilon(1 - \frac{n-1}{n+1}) = \epsilon\frac{2}{n+1}$, but $y_u = 0$ identically. In principle, a more extensive higher-order calculation is necessary to determine the stability properties of this fixed point; however, we can also infer it from topological considerations, i.e. by connecting integral curves knowing the stability properties of the other three fixed points. We will return to this after discussing the final two fixed points.

(3) This third case, as well as the fourth, arise from the nontrivial solution of the quadratic equation for u; both u and $v \neq 0$. The location of the fixed point is:

$$\begin{cases} w &= \epsilon\dfrac{7(3+n)\Delta_1^2 + (n-1)\sqrt{\Delta_1^2(49\Delta_1^2 - 40\Delta_2^2)}}{8\Delta_1^2(5\Delta_2^2(n-1)^2 + 49\Delta_1^2(n+1))} \\ u &= \epsilon\dfrac{49\Delta_1^2 + 10(n-1)\Delta_2^2 - 7\sqrt{49\Delta_1^4 - 40\Delta_1^2\Delta_2^2}}{8\Delta_2^2(49(n+1)\Delta_1^2 + 5(n-1)^2\Delta_2^2)} \end{cases} \tag{7}$$

From this, we obtain the critical exponents:

$$\begin{cases} y_w &= -\epsilon \\ y_u &= \epsilon\dfrac{-49(n-1)\Delta_1^2 + 40(n-1)\Delta_2^2 - 7(n+3)\sqrt{\Delta_1^2(49\Delta_1^2 - 40\Delta_2^2)}}{-98\Delta_1^2(n+1) - 10(n-1)^2\Delta_2^2} \end{cases} \tag{8}$$

(4) This fourth case is obtained from taking the other sign in the quadratic equation for u. The location of this fixed point is given by:

$$\begin{cases} w &= \epsilon\dfrac{7(3+n)\Delta_1^2 - (n-1)\sqrt{\Delta_1^2(49\Delta_1^2 - 40\Delta_2^2)}}{8\Delta_1^2(5\Delta_2^2(n-1)^2 + 49\Delta_1^2(n+1))} \\ u &= \epsilon\dfrac{49\Delta_1^2 + 10(n-1)\Delta_2^2 + 7\sqrt{49\Delta_1^4 - 40\Delta_1^2\Delta_2^2}}{8\Delta_2^2(49(n+1)\Delta_1^2 + 5(n-1)^2\Delta_2^2)} \end{cases} \tag{9}$$

In this case, the critical exponents are:

$$\begin{cases} y_w &= -\epsilon \\ y_u &= \epsilon \dfrac{-49(n-1)\Delta_1^2 + 40(n-1)\Delta_2^2 + 7(n+3)\sqrt{\Delta_1^2(49\Delta_1^2 - 40\Delta_2^2)}}{-98\Delta_1^2(n+1) - 10(n-1)^2\Delta_2^2} \end{cases} \tag{10}$$

One of the interesting features of these last two fixed points is that they only exist for $7\Delta_1^2 \geq 2\sqrt{10}\Delta_2^2$. In terms of initial variables, this translates to the requirement that r not become too positive: $r \leq (7/2\sqrt{10} - 1)(t + K\Lambda^2)$.

With these exponents in hand, we investigate the stability properties of the RG flow in the $u - v$ plane. There are several cases to consider: we will treat only the simplest. First, take $\epsilon = 1$, as this corresponds to a case of great physical interest: a 3-dimensional space. For concreteness, we take $r = 0$, although it is clear that the following topological results are unchanged as long as r is small enough. In this case, we obtain for the last two fixed points the condition for stability

$$\sqrt{49 - 40(\Delta_2/\Delta_1)^2} \geq \pm\frac{7(n+3)}{n-1} \Rightarrow \frac{n-1}{n+3} \geq \pm\frac{7}{3} \tag{11}$$

where the + refers to case (4), the − to case (3). Clearly the $u-$direction for (3) is always unstable, that for (4) is always stable in this limit. For a specific configuration, we can then draw a qualitative version of the RG flow in the $u - w$ plane, as seen in the figure.

FIGURE 3. RG Flow in the $u - w$ plane. This is a qualitative representation of results for $r = 0$. We have also determined the stability of point (2) in the u-direction by considering that otherwise, (4) could no longer be completely stable. For an illustration of how the opposite case breaks down (necessitating a discontinuity in the vector field) see the Appendix.

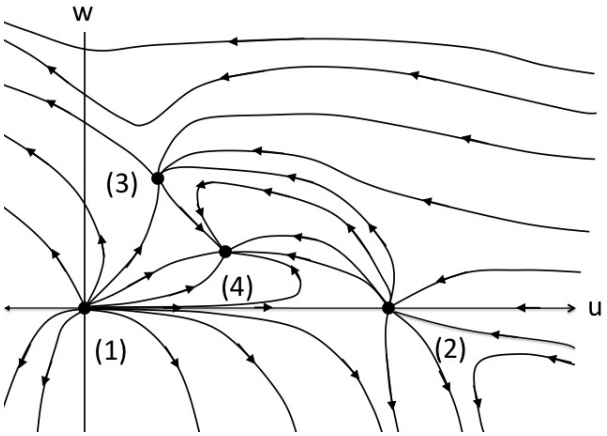

We also return to the new critical temperature(s). Reinterpreting our results as an infinitesimal rescaling, and introducing the symbol $k = t + r$, we see that $t' = b^2\tilde{t}$ and similarly for k. By integrating only over a small shell in our previous expressions for the correction to t and k we get a product of contributions each with one term linear in δl; keeping linear terms, we obtain the recursion relations:

$$\begin{cases} \dfrac{dk}{dl} &= 2k + \left\{ \dfrac{(4u+2v)(n-1)}{K\Lambda^2 + k} + \dfrac{8u+6v}{K\Lambda^2 + t} \right\} K_d\Lambda^d \\ \dfrac{dt}{dl} &= 2t + 2\left\{ \dfrac{(4u+v)(n-1)}{K\Lambda^2 + t} + \dfrac{2u+v}{K\Lambda^2 + k} \right\} K_d\Lambda^d \end{cases} \tag{12}$$

Linearizing about (4), we obtain a quite complicated relation, which can be simplified by placing (perhaps too much) faith in the ϵ-expansion and self-consistently truncating $O(\epsilon^2)$ terms. We get:

$$\begin{aligned} y_t &= 2 - \epsilon((n-1)(\Delta_2^2(\sqrt{\Delta_1^2(49\Delta_1^2 - 40\Delta_2^2)}(n-22) - 30\Delta_2^2(n-1)) - 7\Delta_1^4(10+n) \\ &+ \Delta_1^2(\sqrt{\Delta_1^2(49\Delta_1^2 - 40\Delta_2^2)}(n-8) - \Delta_2^2(158+17n)))/(8\Delta_1^2(5\Delta_2^2(n-1)^2 + 49\Delta_1^2(n-1))) \\ y_k &= \epsilon \times above \end{aligned}$$

i.e. the ϵ coefficients (call them $-T$ and T) in each eigenvalue differ only by a sign. Clearly we expect each of these to be relevant. Note that these are pure numbers; however they depend on the ratio r/t,

$K\Lambda^2/t$, and n. The entrance of Λ^2 should not be frightening; K must be empirically determined; we can absorb Λ into a definition of a new constant K' (with different dimensions). Note that the appearance of r in addition to t is what distinguishes this from the more familiar "cubic anisotropy" case, in which all parameters but n cancel from the final expressions for the exponents [1]. Motivated by the fact that the first carries the 2, we identify it with y_t as labeled. With this in hand, we conclude (again keeping only first-order in ϵ terms):

$$\begin{cases} \nu &= \dfrac{1}{y_t} = \frac{1}{2} + \frac{\epsilon T}{8} \\ \alpha &= 2 - d\nu = 2 - (4-\epsilon)\nu = \frac{\epsilon}{2}(1-T) \end{cases} \tag{13}$$

4. Connections with Experiment & Literature

There are many connections to be made with experiment. The simplest involve a retreating to special cases of our general analysis, for instance $r = 0$, $u = 0$, $v = 0$, and other extremal cases. Note that in many ways this model is similar to the thoroughly investigated "cubic anisotropy" model, for which an ϵ^5 expansion has been performed [3], and which has been realized in several experiments, e.g. [5] and [6]. It also bears similarity to several models discussed by Mukamel and Krinsky [4], who take a similar approach to that of this paper. There, they find that only a few models are stable, i.e. physically realizable–given our results, we expect this variant to fall into that category. Hence one may wish to compare to experimental results, e.g. [2], where a crystal anisotropy of $Fe_{14}Nd_2B$ is extracted from experiment by assuming an Arrott-Noakes equation of state. Other theoretical explanations are then presented; the conclusion is that $\gamma = 1.17 \pm 0.02$ when $\vec{h} \parallel \hat{e}_1$ for such a system [2]. By including an external magnetic field, with trivial renormalization, and applying the relation $\gamma = (2y_h - d)/y_t$, we can determine

$$\gamma = 1 + \epsilon\frac{T}{4}. \tag{14}$$

In principal, we could attempt to fit our result (with $n = 3$) to these data; however, we would need a procedure for determining the ratios of r and K' to t. This could be done by investigating the mean-field phase diagram and comparing transitions; we would incur an error to first-order in u and v by matching this do the mean-field diagram. However, this analysis is not included as it would represent a deviation from the main thread of this inquiry.

5. Conclusion

As we have seen, there are four fixed points arising in the $u - w$ plane upon expanding in ϵ, two of which cease to exist if r becomes too large. One of these is stable whenever it exists. We have also derived critical exponents at this order. While our analysis was fairly general, there are many ways in which it remains unsatisfactory. One would, for instance, like to explicitly compute to second-order in ϵ to see that our conclusion of fixed point 2's stability holds analytically. If not, this could be a signal that the ϵ-expansion's mysteriously strong convergence properties fail in this case. One would also like to keep track of z; it is this parameter in particular that will help to make a connection with the cubic anisotropy model; this seems essential as a verification for these results. For future convenience, we left z as potentially nonzero at the beginning of the *RG* procedure, although we did not write such a Hamiltonian explicitly. Another useful check on these results would be to compare them to the (much longer) formulas obtained by using our neglected renormalization labeling of determining $u + v$ as the coefficient of terms of the form $m_1^2 m_i^2$ for $i \neq 1$, instead of m_1^4. Moreover, by introducing different renormalizations z and z' for m_i ($i \neq 1$) and m_1, a more careful interpretation of our results could determine the dependence of γ, α, and η on $\vec{m} \cdot \vec{h}$; this is done by noting that we should expect only one physical "critical temperature" and adjusting the definitions of field component magnitudes accordingly. Finally, one might notice that our results were fully investigated for only a few cases and values of the parameters at our disposal. There are most likely interesting phenomena yet to be unpacked from our general discussion; this, as well as experimental verification, may prove fruitful for future investigation.

6. Appendix

We carry out the RG for t and r to first order in u and v. Begin with the coarse-graining: change the lattice spacing a to a larger one $a \to ba$ with $b > 1$. I.e. the high-momentum cutoff $\Lambda \sim 1/a$ becomes $\Lambda \to \Lambda/b$ under rescaling; we separate the effects of high and low momenta on the fields via the definition

$$\vec{m}(q) = \begin{cases} \tilde{m}(q) & \text{if } 0 \leq q \leq \Lambda/b; \\ \sigma(q) & \text{if } \Lambda/b < q \leq \Lambda. \end{cases}$$

The original partition function can be written in terms of these separated modes (suppressing vectorial nature of the fields). We also introduce the notation $\int \text{đ}q = \int d^d q/(2\pi)^d$:

$$Z = \int \mathcal{D}\tilde{m}(q^<)\mathcal{D}\sigma(q^>) Exp[-\int_0^{\Lambda/b} \text{đ}q \frac{K(q)}{2}|\tilde{m}(q)|^2] \times Exp[\delta f_b^0] \times \langle Exp[-\mathcal{U}[\tilde{m},\sigma]]\rangle_\sigma$$

and this last we can simply define to be equal to $\int \mathcal{D}\tilde{m}(q) Exp[-\beta\mathcal{H}[\tilde{m}]]$. Therefore the nonconstant contribution to the Hamiltonian is given by

$$+\int_0^{\Lambda/b} \text{đ}q \frac{K(q)}{2}|\tilde{m}(q)|^2 - ln\left\langle e^{-\mathcal{U}}\right\rangle_\sigma .$$

We need zeroth-order two-point functions, which can be read from the Gaussian form of the Hamiltonian:

$$\begin{aligned}\langle m_1(q)m_1(q')\rangle_0 &= \frac{(2\pi)^d\delta(q+q')}{Kq^2+r+t} \\ \langle m_i(q)m_i(q')\rangle_0 &= \frac{(2\pi)^d\delta(q+q')}{Kq^2+t}, (i\neq 1)\end{aligned}$$

Putting aside diagrams, we proceed via a straightforward application of Wick's Theorem. This is a correction to the two-point correlation function; since our results are all independent of q (in particular, not $\propto q^2$) they are purely corrections to t or $t+r$. Since only identical field components are correlated, it follows that there are only two distinct cases to consider: field component 1 and others. In the first case,

$$\begin{aligned}\langle m_1(q)m_1(q')\rangle_1 &= \langle m_1(q)m_1(q')\rangle_0 \\ &- \int \text{đ}q_1\text{đ}q_2\text{đ}q_3 \langle m_i(q_1)m_i(q_2)m_j(q_3)m_j(-q_1-q_2-q_3)m_1(q)m_1(q')\rangle_0 \times (u+\delta_{i1}v)\end{aligned}$$

We take the terms of the correction, given by Wick's theorem, by considering all possible ways of pairing every term in the sum (i.e. omitting disconnected diagrams) and replacing it by the zeroth order two-point correlation function. For notational convenience, we consider first the terms that come from contracting the external legs with signs of the same index:

$$\begin{aligned}\text{same index contractions} &= -2\int \text{đ}q_1\text{đ}q_2\text{đ}q_3 \frac{(2\pi)^d\delta(q_1+q')}{Kq^2+r+t}\frac{(2\pi)^d\delta(q_2+q')}{Kq'^2+r+t} \times \\ &\times \frac{(2\pi)^d\delta(-q_1-q_2)}{t+\delta_{1j}r+Kq_3^2}\delta_{i1}\delta_{i1}\delta_{ij}(u+v\delta_{i1}) + (i\leftrightarrow j; \text{external indices fixed}) \\ &= -\int \text{đ}q_1\text{đ}q_2\text{đ}q_3 \frac{(2\pi)^d\delta(q_1+q')}{Kq^2+r+t}\frac{(2\pi)^d\delta(q_2+q')}{Kq'^2+r+t}(2\pi)^d\delta(-q_1-q_2) \times \\ &\times \left\{\frac{1}{Kq^2+r+t}+\frac{n-1}{Kq^2+t}\right\}(2(u+v)+2u) \\ &= \frac{(2\pi)^d\delta(q+q')}{Kq^2+t+r}\frac{4u+2v}{Kq^2+t+r}\int \text{đ}k\left\{\frac{n-1}{Kk^2+t}+\frac{1}{Kk^2+t+r}\right\}\end{aligned}$$

As the argument is similar, we quote the result for contractions of two different internal indices with external legs. In this case, there is no trace factor and we obtain

$$\text{opposite index pairings} = -\frac{4(u+v)(2\pi)^d\delta(q+q')}{(Kq^2+t+r)^2}\int \text{đ}k \frac{1}{Kk^2+t+r}$$

Adding these leads to the total first-order correction to t. Similarly, the correction to the two-point propagator of, e.g. m_2, is

$$\begin{aligned}\delta\langle m_2(q)m_2(q')\rangle_1 &= -2\frac{(2\pi)^d\delta(q+q')}{(Kq^2+t)^2} \times \\ &\times \int \text{đ}k\left\{\frac{(4u+v)(n-1)}{Kk^2+t}+\frac{2u+v}{Kk^2+t+r}\right\}\end{aligned}$$

This concludes the calculation of critical temperatures. Below, we include both a qualitative plot of the RG flow if one assumes that fixed point (2) is completely unstable, as well as a representative plot using Mathematica.

FIGURE 4. The defective possibility for integral curves of the $u - w$ RG flow. Clearly complete instability of (2) and (1) coupled with complete stability of (4) necessitates a singularity of the vector field below point (4). The only other way out would be to discover a new fixed point below (4); this is indeed possible at higher order in ϵ, so our analysis should be considered only preliminary.

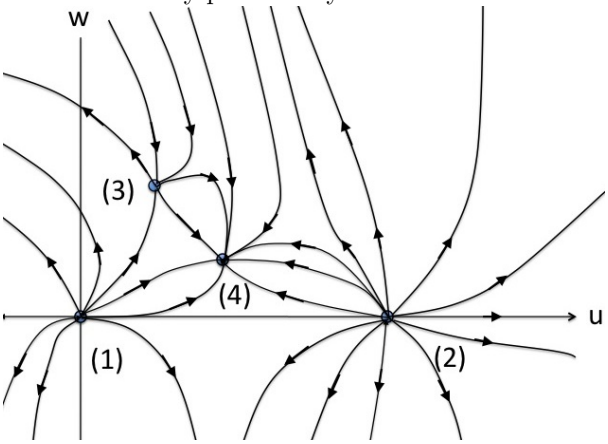

FIGURE 5. RG Flow around origin, as plotted by Mathematica. In this diagram, w is plotted on the lower axis. The specific choice of parameters displayed here is $\epsilon = 0.1$; $\Delta_1^2 = 1$, $\Delta_2^2 = 1.1$. All arrows on integral curves represent flows to the IR. Note that there is difficulty in plotting integral curves in the region between fixed points 1,2, and 3; however, they are clearly visible, as is the fact that fixed point (2) has a stable direction.

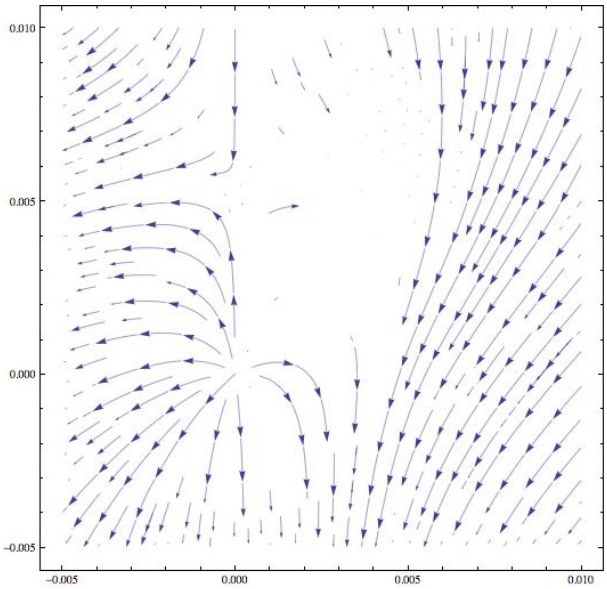

[1] M. Kardar, Statistical Physics of Fields (2007)
[2] D. Kohler and H. Knronmuller, Journal of Magnetism and Magnetic Materials 92, 344 (1990)
[3] R. Guida and J. Zinn-Justin, J. Phys. A 31, 8130 (1998)
[4] D. Mukamel and S. Krinsky, J. Phys. C 8, L496 (1975)
[5] J.A. Lipa, D.R. Swanson, J. Nissen, T.C.P. Chui, and U.E. Iraelson, Phys. Rev. Lett. 76, 944 (1996)
[6] J. Adler, J. Phys. A 16, 3585 (1983)